Received Date : 07-Nov-2016 Revised Date : 29-Jan-2017 Accepted Date : 06-Feb-2017 Article type : Research Report

*In vivo* bioluminescence imaging of neurogenesis: the role of the blood brain barrier in an experimental model of Parkinson's disease

Inga B. Fricke<sup>1,5,†</sup>, Sonja Schelhaas<sup>1</sup>, Bastian Zinnhardt<sup>1,5</sup>, Thomas Viel<sup>1,5,‡</sup>, Sven Hermann<sup>1</sup>, Sébastien Couillard-Després<sup>2,3,5</sup>, Andreas H. Jacobs<sup>1,4,5</sup>.

<sup>1</sup>European Institute for Molecular Imaging (EIMI), University of Münster, Münster, Germany.

<sup>2</sup>Spinal Cord Injury and Tissue Regeneration Center Salzburg (SCI-TReCS), Paracelsus Medical University, Salzburg, Austria.

<sup>3</sup>Institute of Experimental Neuroregeneration, Paracelsus Medical University -Salzburg, Austria <sup>4</sup>Department of Geriatrics and Neurology, Johanniter Hospital, Bonn, Germany.

<sup>5</sup>Imaging Neuroinflammation in Neurodegenerative Diseases (INMiND) EU FP7

consortium.

This article has been accepted for publication and undergone full peer review but has not been through the copyediting, typesetting, pagination and proofreading process, which may lead to differences between this version and the Version of Record. Please cite this article as doi: 10.1111/ejn.13540

<sup>†</sup>Present address: Image-Guided Therapy and Bioengineering Research Group, Institute of Biomaterials & Biomedical Engineering, University of Toronto, 101 College Street, Toronto, ON M5G 1L7, Canada.

<sup>‡</sup>Present address: PARCC, Inserm UMR 970, Université Paris Descartes, 56 rue Leblanc, 75015 Paris, France.

Corresponding author:

Prof. Andreas H. Jacobs, MD European Institute for Molecular Imaging Waldeyerstraße 15 D-48149 Münster Germany ahjacobs@uni-muenster.de Tel. +49 251 83 49300 Fax. +49 251 83 49313

Proposed Journal section: Clinical and Translational Neuroscience Running title: BLI of neurogenesis and the role of the BBB

Keywords: Optical Imaging, Magnetic Resonance, Neurodegeneration, Doublecortin, Substrate Delivery

### **ABSTRACT:**

Bioluminescence imaging in transgenic mice expressing firefly luciferase in Doublecortin<sup>+</sup> (Dcx) neuroblasts might serve as a powerful tool to study the role of neurogenesis in models of brain injury and neurodegeneration using non-invasive,

longitudinal *in vivo* imaging. Therefore, we aimed to use BLI in B6(Cg)-Tyrc-2J/J Dcx-Luc (Doublecortin-Luciferase, Dcx-Luc) mice to investigate its suitability to assess neurogenesis in a unilateral injection model of Parkinson's disease. We further aimed to assess the blood brain barrier leakage associated with the intranigral 6-OHDA injection to evaluate its impact on substrate delivery and bioluminescence signal intensity. 2 weeks after lesion, we observed an increase in bioluminescence signal in the ipsilateral hippocampal region in both, 6-OHDA and vehicle injected Dcx-Luc mice. At the same time, no corresponding increase in Dcx<sup>+</sup> neuroblast numbers could be observed in the dentate gyrus of C57BI6 mice. Blood brain barrier leakage was observed in the hippocampal region and in the degenerating substantia nigra of C57BI6 mice *in vivo* using T1 weighted Magnetic Resonance Imaging with Gadovist<sup>®</sup> and *ex vivo* using Evans Blue Fluorescence Reflectance Imaging and mouse Immunoglobulin G staining. Our data suggests a BLI signal dependency on blood brain barrier permeability, underlining a major pitfall of substrate/tracer dependent imaging in invasive disease models.

#### INTRODUCTION

Adult neurogenesis, the life-long process in which new nerve cells are generated in the brain, is an intriguing target for restoring neurologic function after injury. It mainly takes place in two distinct regions: the dentate gyrus (DG) of the hippocampus generating new dentate granule cells, and the subventricular zone (SVZ) lining the lateral ventricles and generating new neurons for the olfactory bulb (Ming & Song, 2011). During neurogenesis, neural stem cells give rise to neuroblasts expressing the marker Doublecortin (Dcx) until their final differentiation into mature neurons.

Numbers of Dcx<sup>+</sup> cells were shown to correlate with the rate of neurogenesis (Couillard-Despres *et al.*, 2005), allowing the use of Dcx as a marker to study modulation of neurogenesis in disease models and to test pharmacological interventions targeting neurogenesis.

Altered rates of neurogenesis were observed in several neurologic disease models, e.g. increased neurogenesis following cerebral ischemia and traumatic brain injury (Ruan *et al.*, 2014). In neurodegenerative diseases such as Alzheimer's, Parkinson's and Huntington's disease (AD, PD, HD, respectively), several reports describe alterations in neurogenesis, varying from increased or unchanged (Fricke *et al.*, 2016) neurogenic rates, to decreased rates (Ruan *et al.*, 2014).

To study the role of neurogenesis in brain injury and neurodegeneration, approaches using non-invasive, longitudinal *in vivo* imaging are particularly attractive. Approaches enabling the study of adult neurogenesis non-invasively include positron emission tomography (PET) with the tracer 3'-deoxy-3'-[<sup>18</sup>F]fluorothymidine ([<sup>18</sup>F]FLT), Magnetic Resonance Imaging (MRI) with *in situ* iron oxide particle labelling or genetic MRI reporter genes, and optical imaging (bioluminescence and fluorescence) using viral vectors or transgenic animals for reporter gene delivery and expression (Couillard-Despres *et al.*, 2011; Fricke *et al.*, 2016).

Compared to other imaging approaches, bioluminescence imaging (BLI) in transgenic mice expressing firefly luciferase (Luc) in Dcx positive neuroblasts might serve as a powerful tool to assess neurogenesis in a specific, sensitive and at the same time cost- and time-effective way.

However, as BLI is dependent on reproducible substrate delivery to the brain, standardized imaging protocols (Aswendt *et al.*, 2013) and conditions with unimpaired blood brain barrier (BBB) are of crucial importance. Consisting of

endothelial cells, connected by tight junctions and surrounded by astrocytes and pericytes, the BBB restricts the passage of molecules from the blood stream into the interstitial space of the brain (Abbott *et al.*, 2010). Besides being actively transported, substances enter the brain by passive diffusion, which is highly dependent on the size and hydrophilicity of the given substance. In the bioluminescence reaction, the substrate D-Luciferin is oxidized in an ATP-dependent manner by the firefly luciferase enzyme, leading to light emission. This light emission is linearly correlated with the amount of Luciferase if the substrate is present in excess (de Wet *et al.*, 1987). A biodistribution study with [<sup>123</sup>I]iodo-D-Luciferin demonstrated that only a small fraction of D-Luciferin reaches the brain, thereby limiting the BLI signal that is generated in the brain (Lee *et al.*, 2003) and making it vulnerable to differences in substrate distribution due to increased BBB permeability.

This study aimed to use BLI in B6(Cg)-Tyrc-2J/J Dcx-Luc (Dcx-Luc) mice to investigate its suitability to assess neurogenesis in a unilateral injection model of Parkinson's disease (PD). We further aimed to assess the BBB leakage that is associated with intranigral 6-OHDA lesion in order to evaluate its impact on substrate delivery to the brain and the resulting BLI signal.

#### MATERIALS AND METHODS

#### **Animal experiments**

All animal experiments were performed in accordance with the German laws for animal protection and were approved by the local bureau for animal care (LANUV, Landesamt für Natur, Umwelt und Verbraucherschutz Nordrhein-Westfalen). Experiments have been performed and reported in compliance with the ARRIVE guidelines. C57Bl6 (Janvier, Saint-Berthevin, France) and B6(Cg)-Tyrc-2J/J Dcx-Luc mice (Dcx-Luc; provided by S. Couillard-Després, Paracelsus Medical University, Salzburg, Austria) were housed at constant temperature (23 °C) and relative humidity (40 %), under a 12h light / 12h dark schedule. Mice were given *ad libitum* access to food and water.

#### Parkinson's disease model

Stereotactic injections were performed as previously described (Fricke *et al.*, 2016). Briefly, female C57Bl6 (n = 42) and Dcx-Luc (n = 25) mice (12-14 weeks of age) were anaesthetised with ketamine/xylazine (i. p.) and a stereotactic injection of 2 µl 5 mg/ml 6-OHDA (Sigma-Aldrich) in 0.01 % ascorbic acid (Carl Roth, Karlsruhe, Germany) and 0.9 % NaCl (Carl Roth) or vehicle (0.01 % ascorbic acid in 0.9 % NaCl) was performed into the left SN (coordinates in relation to bregma: lateral -1.5 mm, anterior-posterior -3.0 mm, dorsal-ventral -4.4 mm).

#### Single Photon Emission Computed Tomography (SPECT)

SPECT imaging was performed at 7 weeks post injection in 6-OHDA (n = 5) and vehicle (n = 3) injected Dcx-Luc mice that were followed longitudinally with BLI. Imaging and data analysis were performed as described previously (Fricke *et al.*, 2016). Briefly, animals were anaesthetised with 1.5 % isoflurane (Abbott Animal Health, Illinois, USA) in 100 % O<sub>2</sub>, the lateral tail vein was cannulated using a 26 Ga catheter (Vasculon Plus, BD, Heidelberg, Germany), 16 MBq [<sup>123</sup>I]loflupane (N- $\omega$ -fluoropropyl-2 $\beta$ -carbomethoxy-3 $\beta$ -(4-[<sup>123</sup>I]iodophenyl)nortropane, DaTscan<sup>TM</sup>, GE Healthcare, Chalfont St Giles, GB) were injected i. v. and a 15 min SPECT scan was conducted 60 min post injection (p. i.) in a combined SPECT/CT imaging system (NanoSPECT/CT preclinical camera; Mediso Medical Imaging Systems, Budapest, Hungary), followed by a CT acquisition. Images were reconstructed by an orderedsubsets expectation maximization algorithm software (HiSPECT™; SciVis GMBH, Göttingen, Germany).

Image data analysis of SPECT/CT data was performed using the Inveon<sup>™</sup> Research Workplace software package (Siemens Healthcare, Erlangen, Germany). Volumes of interest (VOIs) of equal size and orientation were applied to the right striatum and the cerebellum. A 50 % threshold of the VOI maximum was applied to the VOI for right striatum, and the resulting VOI50 %<sub>right</sub> was mirrored to the left brain hemisphere in order to quantify the left striatum (VOI50 %<sub>left</sub>). Tracer uptake was quantified as mean specific tracer uptake ([mean uptake striatum50 %<sub>left/right</sub> – mean uptake cerebellum] / mean uptake cerebellum) and the specific uptake ratio left/right was calculated. A value below 0.2 was taken as a criterion for successful degeneration. Representative images in Fig. S2 show SPECT/CT images.

#### **Bioluminescence Imaging**

BLI was performed before lesion and either weekly from week two till week seven post lesion ( $n_{6-OHDA} = 5$ ;  $n_{vehicle} = 3$ ; data presented in Fig. 1) or at week 2 post lesion ( $n_{6-OHDA} = 7$ ;  $n_{vehicle} = 7$ ; data presented in Fig. 6) using the IVIS Spectrum Imaging System and Living Image 4.0 software (PerkinElmer, Waltham, MA, USA). The day before measurement, depilatory cream (Pilca) was used to remove the fur on the head under isoflurane anaesthesia. Mice were injected i. p. with 300 mg/kg Dluciferin in phosphate buffered saline (PBS) without calcium and magnesium (PAA Laboratories). 3 min post D-luciferin injection, mice were anaesthetised with 2.5 % isoflurane in 100 % oxygen and placed in the imaging system before 14 acquisitions of 60 sec were recorded between 6 and 20 min p. i. (field of view (FOV): B, subject

height: 1.5 cm, binning: 4, f/stop: 1). Grayscale photographic images and bioluminescence colour images were superimposed. Regions of interest were drawn for the right and left OB, SVZ and DG to determine the signal intensity (Average Radiance [p/s/cm<sup>2</sup>/sr]) and are shown in Supplementary Figure S1. The time frame with the maximal brain bioluminescence signal was chosen for quantification.

### Magnetic Resonance Imaging (MRI)

MRI was performed in C57BI6 mice injected with 6-OHDA (n = 20), vehicle (n = 19), or healthy animals (n = 5) at various time points, as summarized in Supplementary Table S1. In Dcx-Luc animals ( $n_{6-OHDA} = 7$ ,  $n_{vehicle} = 7$ ), MRI images were acquired at 14 days post lesion. To assess BBB leakage with MRI, mice were anaesthetized and catheters were placed as described for the SPECT protocol. A T2 FSE 2D sequence (repetition time/echo time 5253 ms/88.5 ms, 24 slices, slice thickness 0.8 mm, spacing between slices 0.9 mm) and a T1 SE 2D sequence (repetition time/echo time 500 ms/12.4 ms, 20 slices, slice thickness 0.8 mm, spacing between slices 0.9 mm) and a T1 SE 2D sequence (repetition time/echo time 500 ms/12.4 ms, 20 slices, slice thickness 0.8 mm, spacing between slices 0.9 mm) were acquired in a nanoScan PET/MRI scanner equipped with an MH20 coil (Mediso Medical Imaging Systems). Gadovist<sup>®</sup> (Bayer Vital GmbH, Leverkusen, Germany) was injected via the catheter (50 µmol/kg) and a post-Gd T1 sequence was acquired. MRI data were analysed using the in-house built software MEDgical.

#### **Evans Blue Application and Imaging**

Following the final MRI scan, C57Bl6 ( $n_{6-OHDA} = 20$ ,  $n_{vehicle} = 19$ ,  $n_{Healthy} = 5$ ) and Dcx-Luc mice ( $n_{6-OHDA} = 7$ ,  $n_{vehicle} = 7$ ) were kept under isoflurane anaesthesia and 4 µl/g bodyweight of a 4 % Evans Blue (EB; Sigma-Aldrich) solution in 0.9 % NaCl were injected via the catheter. After a circulation time of 30 min, animals were

transcardially perfused with 0.9 % NaCl followed by 4 % PFA and brains were explanted. Photographic images and fluorescence images of the whole brain as well as 2 mm thick coronal slices (sliced with a Stainless Steel Coronal Brain Matrix, Mouse, Slice Width 2 mm (Harvard Apparatus, Holliston, MA, USA)) were acquired from both sides. Photographic images were acquired using a Nikon SMZ800 stereomicroscope equipped with a Nikon SS-2Mv camera.

EB fluorescence was quantified using an IVIS Spectrum Imaging System and Living Image 4.0 software (Filter: excitation 675 nm, emission 720 nm; auto exposure, f/stop: 2, binning: 2, FOV: B, subject height: 5 mm (whole brain) / 0 mm (brain slices)). ROIs of equal size and shape were drawn for the left and right dentate gyrus and substantia nigra and radiant efficiency values ([p/s/cm<sup>2</sup>/sr]/[µW/cm<sup>2</sup>]) were quantified.

Brain slices were post fixed in 4 % PFA and processed for immunohistochemistry.

#### Immunohistochemistry

Following post fixation, the thick brain slices were embedded in paraffin and 5  $\mu$ m thick coronal sections were cut. Sections were deparaffinised, rehydrated and boiled in citrate buffer (pH6 at 25 °C) for antigen retrieval. Either immunofluorescence or immunoperoxidase staining was performed based on the protocol described previously (Fricke *et al.*, 2016). The following antibodies were used: Primary: Tyrosine Hydroxylase (Chicken  $\alpha$  TH 1:800, ab76442, Abcam, Cambridge, UK), Doublecortin (Guinea Pig  $\alpha$  Dcx 1:400, AB2253, Millipore, Billerica, MA, USA) and ionized calcium-binding adapter molecule 1 (Iba1) (Rabbit  $\alpha$  Iba1 1 : 250, no. 019-19742, Wako Chemicals, Neuss, Germany); Secondary: Alexa Fluor 488/555 (1:800,

Life Technologies), DSB-X<sup>™</sup> Biotin Goat Anti-Chicken IgG (1:800, Life Technologies).

To stain extravasated mouse Immunoglobulin G (IgG), a biotinylated Goat α Mouse IgG antibody (1:500, B11027, Life Technologies) was applied overnight at 4 °C.

#### Microscopy

Microscopy was performed using a Nikon ECLIPSE Ni-E microscope (fluorescence stainings) and a Nikon ECLIPSE 90i microscope (immunoperoxidase stainings), both operated by the NIS-Elements AR software. Images were processed using the Fiji ImageJ distribution (Schindelin *et al.*, 2012; Schneider *et al.*, 2012). For immunoperoxidase stainings (TH and IgG), the whole brain slice was scanned using a 4x magnification. Contrast was enhanced using the "Enhance Contrast" tool (0 % saturated pixels, no histogram equalization). For fluorescence Dcx stainings, the left and right dentate gyri were scanned in a 20x magnification. For quantification, a dentate gyrus ROI was generated based on the DAPI image and the left/right ratio of the Dcx stained area/DAPI stained area was calculated. Representative images show Z-Stacks in 20x magnification. For Iba1 stainings, the whole brain slice was scanned using a 10x magnification and representative images of the injection tract region spanning the hippocampus were acquired as Z-stacks in 10x magnification and combined to a focused image using the extended depth of focus function.

#### Statistical analysis

Statistical analysis was performed using Sigma Plot 13.0 (Systat Software Inc, San Jose, CA, USA) and Graph Pad Prism 7 (GraphPad Software, La Jolla, CA, USA).

Longitudinal BLI data were subjected to a two-way repeated measurements ANOVA with pairwise multiple comparison procedures (Holm-Sidak method) and mean (*M*) values are displayed. SPECT data, EB fluorescence ratios, and Dcx/DAPI left/right ratios were compared using a Mann-Whitney Rank Sum Test and median (*Mdn*) values are shown. For BLI data that was acquired at two time points, median values are shown and differences in time within a group were analysed using the Wilcoxon Signed Rank Test. A *P*-value below 0.05 was considered as statistically significant.

#### RESULTS

#### In vivo imaging of neurogenesis following 6-OHDA lesion

In order to induce degeneration of the nigrostriatal system, Dcx-Luc mice were unilaterally injected with 6-OHDA (n = 6) or vehicle (n = 4). One vehicle injected animal died during the pre-injection scan and one 6-OHDA injected animal had to be sacrificed due to weight loss ( $\geq 20$  %) following lesion. In order to validate the successful lesion in 6-OHDA injected animals and the integrity of the nigrostriatal system in vehicle injected animals, we used [<sup>123</sup>I]Ioflupane SPECT at week 8 post lesion (Supplementary Figure S2), followed by TH immunohistochemistry (data not shown). Striatal [<sup>123</sup>I]Ioflupane uptake ratios in 6-OHDA compared to vehicle injected animals were significantly decreased ( $Mdn_{6-OHDA} = 0.10$ ,  $n_{6-OHDA} = 5$ ;  $Mdn_{vehicle} = 0.93$ ,  $n_{vehicle} = 3$ , U = 0, P = 0.036, Mann-Whitney Rank Sum Test, Supplementary Figure S2b). Based on our previous experience, we defined a striatal [<sup>123</sup>I]Ioflupane uptake ratio equal to or lower than 0.2 as a criterion for successful degeneration, leading to the exclusion of two animals from the analysis and a group size of n = 3 per group (Supplementary Figure S2c).

BLI measurements were performed before lesion and weekly between week 2 and 7 post lesion (Fig. 1a). In week 1 post lesion, a quantification of BLI signal was not possible due to scar tissue remaining from the surgery. Following injection, vehicle and 6-OHDA injected animals showed no significantly different hippocampus left/right ratios ( $F_{1,41} = 0.114$ , P = 0.752, two way repeated measurements ANOVA). Allowing for differences in group, a significantly increased hippocampus left/right BLI signal ratio (Fig. 1b, e) was observed at 2 weeks compared to the pre lesion condition ( $M_{w0} = 1.01$ ,  $SD_{w0} = 0.03$ ,  $M_{w2} = 1.24$ ,  $SD_{w2} = 0.08$ ,  $t_6 = 7.45$ , P < 0.001, two way repeated measurements ANOVA with pairwise multiple comparison procedures (Holm-Sidak method)), while SVZ and OB signals were unchanged at all time points (Fig. 1b, c, d).

### Potential sources of an increased Dcx-Luc BLI signal

We investigated the expression of Dcx in the dentate gyrus by IHC and the possibility of a facilitated substrate entry to the brain due to BBB leakage induced by our injection procedure by MRI and FRI. C57Bl6 mice received a unilateral injection of 6-OHDA (n = 21) or vehicle (n = 21) into the left substantia nigra and BBB leakage was imaged *in vivo* by Gadovist<sup>®</sup> enhanced T1 weighted MRI and *ex vivo* by FRI of EB extravasation at 2, 7, 14, or 28 days post injection. Two 6-OHDA and one vehicle injected animal died during image acquisition and did not enter the final data analysis. Additionally, 5 healthy C57Bl6 mice were included in the imaging and all brains were processed for IHC.

*Numbers of Dcx<sup>+</sup> cells in the dentate gyrus of C57Bl6 mice following lesion* 

Following injection of 6-OHDA or vehicle, no obvious difference in Dcx staining between the left (ipsilateral) and right (contralateral) dentate gyrus was observed (Fig. 2a). Quantification of Dcx stained area and DAPI stained area showed unchanged left/right ratio of Dcx/DAPI stained area between 6-OHDA and vehicle (Fig. 2b; Mann-Whitney Rank Sum Test). On day 7, a significantly increased left/right ratio was observed in the 6-OHDA injected group compared to the healthy control group. In addition, a significantly increased ratio was observed in the vehicle injected group compared to healthy controls on day 14 and 28 ( $Mdn_{6-OHDA, d7} = 1.72$ , U = 2.0, P = 0.032;  $Mdn_{Vehicle, d14} = 1.36$ , U = 2.0, P = 0.032;  $Mdn_{Vehicle, d14} = 1.36$ , U = 2.0, P = 0.032; Mann-Whitney Rank Sum Test). Taken together, the observed alterations in hippocampal Dcx expression following injection do not follow the same temporal pattern as the BLI signal.

# The intranigral injection procedure leads to blood brain barrier damage in the dentate gyrus region

To investigate whether a facilitated substrate entry could be the basis of the observed BLI signal increase, BBB leakage was assessed in a semi quantitative way by *ex vivo* FRI with EB (Fig. 3a-c). In addition, Gd enhanced T1w MRI and immunostaining for IgG were performed to validate the FRI findings (Fig. 3a). When comparing white light and fluorescence images of EB distribution, we observed a clearer signal using the FRI approach, giving a better image of the regional distribution and concentration of EB and the possibility for quantification (Supplementary Figure S3). In the healthy control group, no EB fluorescence signal or Gd contrast enhancement was observed. In the vehicle injected group, EB and Gd

extravasation was observed along the injection tract, also spanning the hippocampus region. Besides in the injection tract, additional EB and Gd extravasation were observed in the 6-OHDA lesioned SN. At all studied time points, hippocampus left/right FRI signal ratios were not differing significantly between 6-OHDA and vehicle injected group (Fig. 3b). However, the signal ratio in the 6-OHDA injected group was at all time points significantly higher compared to the healthy control group ( $Mdn_{Control} = 1.05$ , n = 5;  $Mdn_{6-OHDA, d2} = 1.37$ , n = 5, U = 0.0, P = 0.008;  $Mdn_{6-OHDA, d7} = 1.32$ , n = 5, U = 0.0, P = 0.008;  $Mdn_{6-OHDA, d14} = 1.26$ , n = 5, U = 2.0, P = 0.032;  $Mdn_{6-OHDA, d28} = 1.40$ , n = 5, U = 0.0, P = 0.008). Additionally, the hippocampus left/right FRI signal ratio in the vehicle group was significantly increased on day 2 ( $Mdn_{Vehicle, d28} = 1.54$ , n = 4, U = 1.0, P = 0.032) and day 28 ( $Mdn_{Vehicle, d28} = 1.25$ , n = 5, U = 0.0, P = 0.008) compared to the healthy control. In conclusion, an increased BBB permeability was observed in the hippocampal region and along the injection tract in both, 6-OHDA and vehicle injected animals.

# Dopaminergic neurodegeneration is accompanied by persistent blood brain barrier opening

Despite the observed BBB leakage along the injection tract, an increased EB and Gd extravasation was observed in the 6-OHDA lesioned SN compared to the vehicle injected or healthy control SN. The SN left/right FRI signal ratio was significantly increased in the 6-OHDA group on day 7, 14, and 28 compared to the vehicle group (Fig. 3c;  $Mdn_{Vehicle, d7} = 0.98$ ,  $Mdn_{6-OHDA, d7} = 1.47$ , n = 5, U = 0.0, P = 0.008;  $Mdn_{Vehicle, d14} = 0.97$ ,  $Mdn_{6-OHDA, d14} = 1.23$ , n = 5, U = 2.0, P = 0.032;  $Mdn_{Vehicle, d28} = 1.11$ ,  $Mdn_{6-OHDA, d28} = 1.59$ , n = 5, U = 0.0, P = 0.008) and on day 2 and day 28 compared to the healthy control group ( $Mdn_{Control} = 1.02$ ;  $Mdn_{6-OHDA, d2} = 1.63$ , n = 5,

U = 1.0, P = 0.016;  $Mdn_{6-OHDA, d28} = 1.59$ , n = 5, U = 2.0, P = 0.032). The successful lesion in the 6-OHDA injected animals as well as the integrity of the nigrostriatal system in vehicle injected animals was proven by TH immunohistochemistry (Fig. 3a). Taken together, a persistent BBB leakage was observed in the 6-OHDA lesioned SN.

#### Intra-individual time course of BBB leakage

In order to investigate the intra-individual time course of BBB opening following intranigral injection of vehicle and 6-OHDA, four animals per group were subjected to repeated MRI measurements on day 2, 14, and 28 p. i. and EB FRI on day 28 (Fig. 4. The observed time course of Gd extravasation in the vehicle group ranges from no visible extravasation (Vehicle 1), over a declining signal in the hippocampal region (Vehicle 2 & 3) to a rather stable signal in the hippocampus (Vehicle 4). In the 6-OHDA lesioned group, a similar distribution is visible, ranging from a persistent BBB damage in the SN and/or injection tract region (6-OHDA 1, 3 & 4) to a declining BBB damage in the SN (6-OHDA 2). For all animals, the last T1w MRI shows a good spatial relation with the EB FRI images obtained on the same day (Fig. 4, FRI A-C).

#### Immune cell activation in areas of blood brain barrier leakage

In order to evaluate the role of the immune cells in the observed blood brain barrier leakage following dopaminergic neurodegeneration and mechanic injury, we performed immunohistochemistry for ionized calcium-binding adapter molecule 1 (Iba1), a marker for microglia/macrophages, at 14 and 28 days post injection of vehicle or 6-OHDA (Fig. 5). An increase in density in Iba1<sup>+</sup> immune cells and a morphological change towards an activated phenotype was observed in areas of BBB leakage around the injection tract, spanning the area of the hippocampus, and the degenerating substantia nigra at all studied time points. At two weeks post lesion, more (activated) microglia were observed. Iba1<sup>+</sup> cells with an activated phenotype were not observed on the contralateral side of the brain.

#### Imaging of blood brain barrier leakage and BLI in Dcx-Luc mice

In order to demonstrate in the same animal that the observed increase in BLI signal is in fact related to an increase in BBB permeability, we injected Dcx-Luc mice with 6-OHDA (n = 9) or vehicle (n = 7) into the substantia nigra and acquired BLI before and two weeks post injection, followed by BBB assessment using Gadovist<sup>®</sup>enhanced T1w MRI and FRI with EB (summarized in Fig. 6a). Two animals were sacrificed due to weight loss ( $\geq$  20 %) following 6-OHDA lesion. As immunohistochemistry for TH revealed that the 6-OHDA lesion did not lead to a complete degeneration of left substantia nigra in 5 out of 7 animals, we only included the data obtained for the vehicle injected group. An increased BLI signal left/right ratio was observed in the hippocampal region of vehicle injected animals at day 14 post injection compared to the pre lesion condition ( $Mdn_{Vehicle, d-1} = 0.98$ ,  $Mdn_{Vehicle, d14}$ ) = 1.20, *n* = 7, *W* = 26, *P* = 0.0313; Wilcoxon Signed Rank Test; Fig. 6a & e). A slight, but significant, increase in BLI signal left/right was also observed in the SVZ  $(Mdn_{Vehicle, d-1} = 0.99, Mdn_{Vehicle, d14} = 1.09, n = 7, W = 26, P = 0.0313, Wilcoxon$ Signed Rank Test, Fig. 6d), compared to the pre lesion condition. No difference was observed for the olfactory bulb (Fig. 6c). Using Gadovist<sup>®</sup>-enhanced T1w MRI, BBB leakage along the injection tract was only observed in two out of 7 vehicle injected

animals. Quantification of the *ex vivo* FRI measurements following EB injection did not show a significant difference between vehicle-injected and healthy control (C57Bl6 from the previous experiment shown in Fig. 3) animals with respect to Hippocampus or SN left/right signal ratios (Hippocampus:  $Mdn_{Vehicle} = 0.99$ ,  $n_{Vehicle} =$ 7,  $Mdn_{Healthy} = 1.05$ ,  $n_{Healthy} = 5$ ; SN:  $Mdn_{Vehicle} = 1.07$ ,  $n_{Vehicle} = 7$ ,  $Mdn_{Healthy} = 1.02$ ,  $n_{Healthy} = 5$ ; Mann-Whitney Rank Sum Test; Fig. 6 f-h). Using immunohistochemistry for IgG, we detected BBB leakage around the injection tract in all vehicle injected mice.

In conclusion, we observed a clear increase in BLI left/right ratio in the hippocampal region in vehicle injected animals at two weeks post lesion, which is accompanied by a weak increase in BBB permeability detectable by IgG immunohistochemistry, but not by contrast enhanced T1w MRI or *ex vivo* FRI following EB administration.

#### DISCUSSION

Following both, intranigral 6-OHDA and vehicle injection in Dcx-Luc mice, we observed a significantly increased BLI signal originating from the ipsilateral hippocampal region at two weeks post lesion, which slowly decreased in the following weeks. This temporal pattern was not recapitulated by the Dcx expression in the ipsilateral dentate gyrus of C57Bl6 mice post 6-OHDA or vehicle injection. Using *in vivo* Gd enhanced T1w MRI, *ex vivo* FRI with EB and IgG immunostaining, an increased BBB permeability was observed in the hippocampal region and along the injection tract in both, 6-OHDA and vehicle injected animals between day 2 and 28. Additionally, a persistent BBB leakage was observed in the 6-OHDA lesioned SN at all studied time points. In the intra-individual comparison, the observed pattern, severity, and timing of BBB disruption was highly variable. In a second set of Dcx-

Luc mice, the increased BLI signal at week two post vehicle injection could be reproduced, even though the BBB leakage observed in these mice was rather weak, as it could only be detected by IgG IHC.

# Expression of the neurogenesis marker Dcx in the dentate gyrus is unchanged following intranigral 6-OHDA application

Even though we found an increased BLI signal in the hippocampal area of Dcx-Luc mice following intranigral injection of 6-OHDA or vehicle, this increase could not be confirmed in the immunohistochemical stainings for Dcx in C57BI6 mice, suggesting that neither the injection procedure nor the nigrostriatal lesion has an effect on hippocampal neurogenesis with regards to total Dcx expression. In contrast, several studies reported a reduction of neurogenesis in the dentate gyrus in experimental models of PD as well as in PD patients, which was linked to dopamine depletion following dopaminergic neurodegeneration. In PD patients, a reduced density of progenitor cells in the DG was reported (Höglinger et al., 2004). A reduced cell proliferation was also described following intranigral 6-OHDA lesion in rats (Suzuki et al., 2010) and mice (Chiu et al., 2015), and in MPTP-lesioned mice (Höglinger et al., 2004). The opposite effect, a transient increase in progenitor cell division, was observed in the DG of MPTP(1-methyl-4-phenyl-1,2,3,6-tetrahydropyridine)-treated animals at 14 days post treatment, but not at 4 or 30 days post treatment (Park & Enikolopov, 2010). Another study reported an increase in new-born Type 2b cells following MPTP treatment, while the absolute number of Type 2b cells was unchanged (Lesemann et al., 2012). The controversial results obtained underline that the use of different markers, marker combinations, and models might result in a different experimental outcome. The increased BLI signal we observed in both, 6OHDA and vehicle injected animals does not seem to be related to an actual increase in hippocampal neurogenesis. In addition to Dcx<sup>+</sup> cells in the hippocampus, Dcx+ cells in the SVZ drive the overall intensity of the observed BLI signal in Dcx-Luc mice. In our second set of Dcx-Luc mice, we observed a very slight increase in BLI left/right signal ratios in the SVZ. This increase might be due to slight scatter from the strong signal in the hippocampal area. We observed previously (Fricke *et al.*, 2016), that neurogenesis in the SVZ is unchanged following intranigral 6-OHDA lesion, indicating that also the neurogenesis in the SVZ is most likely not the source of the increased BLI signal. Hence, the observed alterations in BLI probably result from a different source.

# BBB leakage induced by mechanic injury and dopaminergic neurodegeneration

The source for an increased BLI signal in spite of an unchanged Dcx expression could, at least in part, be an increased substrate availability due to a regional damage of the BBB. We observed a leakage of Gadovist<sup>®</sup>, EB and IgG along the injection tract, also spanning the hippocampus in both, 6-OHDA and vehicle injected C57BI6 animals. This is in line with the finding of FITC-labelled albumin leakage around the injection tract at 10 days post 6-OHDA injection in rats (Carvey *et al.*, 2005). Besides BBB damage due to the injection procedure, we also observed a persistent BBB damage in the 6-OHDA lesioned SN in these animals. In agreement with our results, FITC-labelled albumin leakage was reported in the ipsilateral SN and at the primary 6-OHDA injection site 10 days following striatal 6-OHDA injection in rats (Carvey *et al.*, 2005). In the same study, MFB injections of 6-OHDA resulted in a BBB leakage in SN and striatum at 10 and 34 days post injection (Carvey *et al.*,

2005), indicating that degeneration of dopaminergic cell bodies in the SN and dopaminergic fibres in the striatum induces a long-lasting BBB damage, which was already described by Cooper *et al.* (Cooper *et al.*, 1982). In contrast to our results in C57BI6 mice, we did not observe this increased BBB permeability in vehicle injected Dcx-Luc animals using *in vivo* Gd enhanced T1w MRI and *ex vivo* FRI following EB injection. In the immunohistochemical staining for IgG, a moderate extravasation was observed, showing that the degree of BBB impairment can vary between animals and experiments.

In addition to an increased BBB permeability, facilitated light penetration through the hole that is drilled into the skull during the stereotactic injection should be considered as another factor increasing the BLI signal at time points early after injection, likely also impacting the signal we observed at two weeks post lesion.

# Blood brain barrier leakage is associated with microglia/macrophage activation

We previously observed increased numbers and activation of microglia cells close to the injection tract and in the degenerating substantia nigra in our animal model (Fricke *et al.*, 2016), indicating that immune cells might play a role in BBB opening in this model. In agreement with previous results, we observed increased density of Iba1<sup>+</sup> microglia/macrophages in regions of IgG extravasation in the area of the injection tract.

### The blood brain barrier as a limiting factor for substrate availability

The intact BBB restricts diffusion of D-Luciferin into the brain and plays a role in eliminating D-Luciferin from the brain by active transport processes via drug efflux

transporter ABCG2 (ATP-binding cassette subfamily G member 2) (Bakhsheshian *et al.*, 2013). Thereby it notably restricts the availability of substrate in the brain. When increasing amounts of D-Luciferin (15, 150, 300, 750 mg/kg) were applied in healthy Dcx-Luc mice, no saturating photon emission level could be reached (Aswendt *et al.*, 2013), highlighting that D-Luciferin is not present in excess under normal experimental conditions. This observation also holds true for tracer substances in nuclear imaging that possess limited BBB mobility. A biodistribution study of [<sup>125</sup>I]iodo-D-Luciferin and <sup>14</sup>C-D-Luciferin in mice confirmed the very limited brain uptake in mice (<1 %ID/g 5 min post i. p. injection) (Lee *et al.*, 2003; Berger *et al.*, 2008).

A study using an Experimental Autoimmune Encephalomyelitis (EAE) model in Dcx-Luc mice already described an increase in BLI signal unrelated to neurogenesis, which followed the same temporal pattern as the opening of the BBB (Ayzenberg *et al.*, 2015). Nevertheless, more research is needed to determine the impact of BBB alterations on substrate/tracer availability in different models and diseases.

The necessity of BBB assessment in substrate/tracer dependent brain imaging To allow for quantification in substrate or tracer dependent brain imaging in conditions that potentially increase BBB permeability, the BBB should be assessed. Various methods to assess BBB leakage exist, including *in vivo* MRI, *ex vivo* FRI with different tracer substances, and histological stainings. *Ex vivo* fluorescence imaging of EB leakage was previously used in a rat model of stroke (Jaffer *et al.*, 2013) and in an approach to open the BBB using low frequency focused ultra-sound (Shen *et al.*, 2014). It was described as more sensitive than the conventional EB approach using white light images of EB distribution or ultraviolet spectrophotometry

(Jaffer *et al.*, 2013). Using the same approach, we could confirm EB FRI as a relatively sensitive, fast and cost-efficient method. Nevertheless, EB FRI is less sensitive than immunohistochemistry for IgG extravasation, is only semi-quantitative, and lacks the option for longitudinal imaging.

#### Limitations of bioluminescence imaging in the brain

Bioluminescence imaging in the brain can be utilized for various purposes, but it also confronts us with a range of different challenges for its proper quantification and interpretation. Its 2D nature and the absorption and scattering of light travelling through tissue make it difficult to define proper regions of interest. In addition, surgical manipulations to the brain and skull like intracranial injection associated with local thinning of the skull after creating a hole for injection might result in a facilitated light penetration leading to an increase in detected BLI signal. Furthermore, increased substrate delivery to the brain due to a disrupted BBB might play a role in several models, including stereotactic injections, neurodegeneration, ischemic events, or tumor development.

#### CONCLUSIONS

An increased BLI signal in the neurogenic regions close to the injection tract was observed in both, 6-OHDA and vehicle injected animals, at 2 weeks post lesion, which was not recapitulated in Dcx<sup>+</sup> cell numbers in the dentate gyrus. In addition, a BBB damage associated with the injection procedure and the ongoing neurodegenerative processes was observed in C57Bl6 mice. In a second set of vehicle-injected Dcx-Luc mice, a weaker BBB leakage was observed. These data suggest, that the measured BLI signals could result from increased substrate

availability due to BBB damage and facilitated light penetration through the impacted skull, rather than a difference in neurogenesis. Our study underlines the importance of BBB assessment in *in vivo* imaging studies based on tracer substances and enzyme substrates with a limited BBB permeability. Furthermore, the variability of BBB damage observed in invasive intracranial injection models has to be taken into account in future studies.

#### **ACKNOWLEDGEMENTS:**

The authors thank C. Bätza, S. Bouma, I. Hoppe, S. Köster, C. Möllmann, R. Priebe, D. Reinhard and P. Zaunmair for their excellent technical support. We also acknowledge the Interdisciplinary Centre for Clinical Research (IZKF, core unit PIX), Münster, Germany for supporting the MR measurements, namely Prof. Dr. Cornelius Faber and Dr. Lydia Wachsmuth. The research leading to these results has received funding from the Interdisciplinary Centre for Clinical Research (IZKF), Münster, Germany (project SchwJ3/001/11 and core unit PIX) and the European Union's Seventh Framework Programme (FP7/2007-2013) under grant agreement n° 278850 (INMiND).

#### CONFLICT OF INTEREST STATEMENT:

The authors declared no conflict of interest.

#### **AUTHOR CONTRIBUTIONS:**

I. B. F. designed the study, conducted the experiments, designed the figures, and drafted the manuscript. S. S. and B. Z. supported data acquisition and interpretation and drafted the manuscript. T. V., S. H., S. C. D. and A. H. J. were involved in data

interpretation and drafted the manuscript. All authors approved the final version of the manuscript.

# DATA ACCESSIBILITY STATEMENT:

Supplementary data associated with this article can be found in the online version. Original data is available from the authors upon request.

1

## **ABBREVIATIONS:**

	BBB	Blood brain barrier
	BLI	Bioluminescence Imaging
	СТ	Computed Tomography
	Dcx	Doublecortin
	Dcx-Luc	B6(Cg)-Tyrc-2J/J Dcx-Luc
	DG	Dentate gyrus
	FRI	Fluorescence Reflectance Imaging
	Gd	Gadolinium
	lba1	Ionized calcium-binding adapter molecule
	lgG	Immunoglobulin G
	i. p.	Intraperitoneal
	i. v.	Intravenous
	Luc	Firefly luciferase
	М	Mean
	Mdn	Median
	MRI	Magnetic Resonance Imaging
	OB	Olfactory bulb

PD	Parkinson's disease	
p. i.	Post injection	
ROI	Region of interest	
SVZ	Subventricular zone	
[ <sup>123</sup> I]loflupane	$N-\omega$ -fluoropropyl-2 $\beta$ -carbomethoxy-3 $\beta$ -(4-	
[ <sup>123</sup> I]iodophenyl)nortropane		
[ <sup>18</sup> F]FLT	3'-deoxy-3'-[ <sup>18</sup> F]fluorothymidine	
6-OHDA	6-hydroxydopamine	

# **REFERENCES:**

- Abbott, N.J., Patabendige, A.A.K., Dolman, D.E.M., Yusof, S.R., & Begley, D.J. (2010) Structure and function of the blood-brain barrier. *Neurobiol. Dis.*, **37**, 13– 25.
- Aswendt, M., Adamczak, J., Couillard-Despres, S., & Hoehn, M. (2013) Boosting Bioluminescence Neuroimaging: An Optimized Protocol for Brain Studies. *PLoS One*, **8**, e55662.
- Ayzenberg, I., Schlevogt, S., Metzdorf, J., Stahlke, S., Pedreitturia, X., Hunfeld, A., Couillard-Despres, S., & Kleiter, I. (2015) Analysis of neurogenesis during experimental autoimmune encephalomyelitis reveals pitfalls of bioluminescence imaging. *PLoS One*, **10**, e0118550.
- Bakhsheshian, J., Wei, B.-R., Chang, K.-E., Shukla, S., Ambudkar, S. V, Simpson, R.M., Gottesman, M.M., & Hall, M.D. (2013) Bioluminescent imaging of drug efflux at the blood-brain barrier mediated by the transporter ABCG2. *Proc. Natl. Acad. Sci. U. S. A.*, **110**, 20801–20806.
- Berger, F., Paulmurugan, R., Bhaumik, S., & Gambhir, S.S. (2008) Uptake kinetics and biodistribution of 14C-D-luciferin--a radiolabeled substrate for the firefly luciferase catalyzed bioluminescence reaction: impact on bioluminescence based reporter gene imaging. *Eur. J. Nucl. Med. Mol. Imaging*, **35**, 2275–2285.

Carvey, P.M., Zhao, C.H., Hendey, B., Lum, H., Trachtenberg, J., Desai, B.S., Snyder, J., Zhu, Y.G., & Ling, Z.D. (2005) 6-Hydroxydopamine-induced alterations in blood-brain barrier permeability. *Eur. J. Neurosci.*, **22**, 1158–1168.

Chiu, W.-H., Depboylu, C., Hermanns, G., Maurer, L., Windolph, A., Oertel, W.H., Ries, V., & Höglinger, G.U. (2015) Long-term treatment with L-DOPA or pramipexole affects adult neurogenesis and corresponding non-motor behavior in a mouse model of Parkinson's disease. *Neuropharmacology*, **95**, 367–376.

Cooper, P.H., Novin, D., & Butcher, L.L. (1982) Intracerebral 6-hydroxydopamine produces extensive damage to the blood-brain barrier in rats. *Neurosci. Lett.*,

**30**, 13–18.

- Couillard-Despres, S., Vreys, R., Aigner, L., & der Linden, A. Van (2011) In vivo monitoring of adult neurogenesis in health and disease. *Front. Neurosci.*, **5**, 67.
- Couillard-Despres, S., Winner, B., Schaubeck, S., Aigner, R., Vroemen, M., Weidner, N., Bogdahn, U., Winkler, J., Kuhn, H.-G., & Aigner, L. (2005) Doublecortin expression levels in adult brain reflect neurogenesis. *Eur. J. Neurosci.*, **21**, 1–14.
- de Wet, J.R., Wood, K. V, DeLuca, M., Helinski, D.R., & Subramani, S. (1987) Firefly luciferase gene: structure and expression in mammalian cells. *Mol. Cell. Biol.*, **7**, 725–737.
- Fricke, I.B., Viel, T., Worlitzer, M.M., Collmann, F.M., Vrachimis, A., Faust, A., Wachsmuth, L., Faber, C., Dollé, F., Kuhlmann, M.T., Schäfers, K., Hermann, S., Schwamborn, J.C., & Jacobs, A.H. (2016) 6-hydroxydopamine-induced Parkinson's disease-like degeneration generates acute microgliosis and astrogliosis in the nigrostriatal system but no bioluminescence imagingdetectable alteration in adult neurogenesis. *Eur. J. Neurosci.*, **43**, 1352–1365.
- Höglinger, G.U., Rizk, P., Muriel, M.P., Duyckaerts, C., Oertel, W.H., Caille, I., & Hirsch, E.C. (2004) Dopamine depletion impairs precursor cell proliferation in Parkinson disease. *Nat. Neurosci.*, **7**, 726–735.
- Jaffer, H., Adjei, I.M., & Labhasetwar, V. (2013) Optical imaging to map blood-brain barrier leakage. *Sci. Rep.*, **3**, 3117.
- Lee, K.-H., Byun, S.S., Paik, J.-Y., Lee, S.Y., Song, S.H., Choe, Y.S., & Kim, B.-T. (2003) Cell uptake and tissue distribution of radioiodine labelled D-luciferin: implications for luciferase based gene imaging. *Nucl. Med. Commun.*, 24, 1003– 1009.
- Lesemann, A., Reinel, C., Hühnchen, P., Pilhatsch, M., Hellweg, R., Klaissle, P., Winter, C., & Steiner, B. (2012) MPTP-induced hippocampal effects on serotonin, dopamine, neurotrophins, adult neurogenesis and depression-like behavior are partially influenced by fluoxetine in adult mice. *Brain Res.*, **1457**, 51–69.
- Ming, G.-L. & Song, H. (2011) Adult neurogenesis in the mammalian brain: significant answers and significant questions. *Neuron*, **70**, 687–702.
- Park, J.H. & Enikolopov, G. (2010) Transient elevation of adult hippocampal neurogenesis after dopamine depletion. *Exp. Neurol.*, **222**, 267–276.
- Ruan, L., Lau, B.W.-M., Wang, J., Huang, L., Zhuge, Q., Wang, B., Jin, K., & So, K. F. (2014) Neurogenesis in neurological and psychiatric diseases and brain injury: from bench to bedside. *Prog. Neurobiol.*, **115**, 116–137.
- Schindelin, J., Arganda-Carreras, I., Frise, E., Kaynig, V., Longair, M., Pietzsch, T., Preibisch, S., Rueden, C., Saalfeld, S., Schmid, B., Tinevez, J.-Y., White, D.J., Hartenstein, V., Eliceiri, K., Tomancak, P., & Cardona, A. (2012) Fiji: an opensource platform for biological-image analysis. *Nat. Methods*, **9**, 676–682.
- Schneider, C.A., Rasband, W.S., & Eliceiri, K.W. (2012) NIH Image to ImageJ: 25 years of image analysis. *Nat. Methods*, **9**, 671–675.

Shen, Y., Zhang, A., Guo, J., Dan, G., Chen, S., & Yu, H. (2014) Fluorescence imaging of Evans blue extravasation into mouse brain induced by low frequency ultrasound with microbubble. *Biomed. Mater. Eng.*, **24**, 2831–2838.

Suzuki, K., Okada, K., Wakuda, T., Shinmura, C., Kameno, Y., Iwata, K., Takahashi, T., Suda, S., Matsuzaki, H., Iwata, Y., Hashimoto, K., & Mori, N. (2010)
Destruction of dopaminergic neurons in the midbrain by 6-hydroxydopamine decreases hippocampal cell proliferation in rats: reversal by fluoxetine. *PLoS One*, **5**, e9260.

#### FIGURE CAPTIONS:

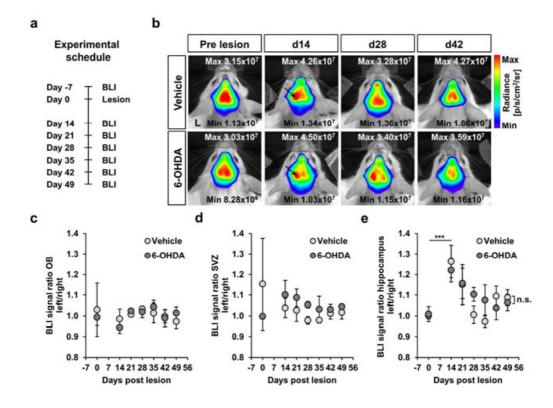
Figure 1: Longitudinal Bioluminescence Imaging in Dcx-Luc mice before and after intranigral injection of 6-OHDA (n = 3) or vehicle (n = 3): (a) Experimental design. (b) Representative BLI images. Arrows point towards the region where an increased BLI signal was observed. (c-e) Quantification of BLI signal left/right ratios for OB (c), SVZ (d) and DG (e). Significance level \*\*\* P < 0.001, day 14 vs. day 0 when allowing for differences in group. 6-OHDA and vehicle are not significantly different (n.s.). Two-way repeated measurements ANOVA with pairwise multiple comparison procedures (Holm-Sidak method).

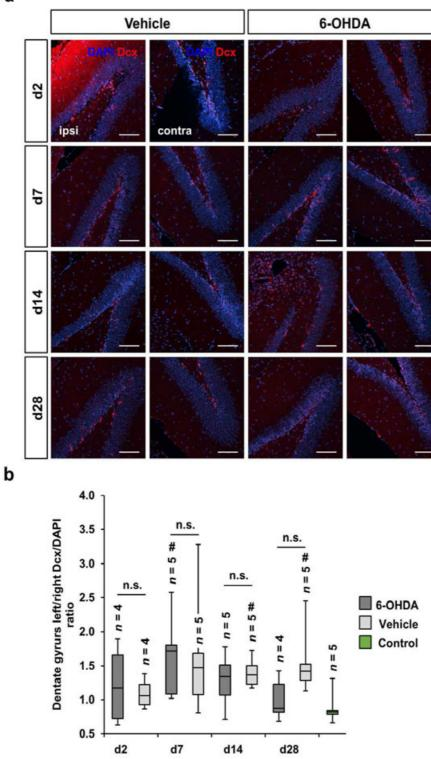
Figure 2: Numbers of Dcx<sup>+</sup> neuroblasts in the dentate gyrus of C57Bl6 mice are unchanged following 6-OHDA lesion: (a) Representative images DAPI/Dcx staining in the ipsi- (left) and contralateral (right) dentate gyrus at 2, 7, 14 and 28 days post vehicle/6-OHDA injection. Scale bar: 100 µm. (b) Quantification of the left/right ratio of Dcx stained area per DAPI stained area. Significance level: \*P < 0.05; \* 6-OHDA/vehicle vs. healthy control; Mann-Whitney Rank Sum Test. Box plot shows median value and upper/lower quartiles. Whiskers display minimal and maximal values obtained.

Figure 3: *In vivo* and *ex vivo* imaging of blood brain barrier leakage following lesion: (a) Representative images of Gadovist<sup>®</sup>-enhanced T1 weighted MRI (MRI + Gd), Evans Blue fluorescence (EB FRI), IgG immunoreactivity (IgG) and tyrosine hydroxylase immunoreactivity (TH) in 6-OHDA- and vehicle-injected animals at day 2, 7, 14 and 28 post injection and in healthy controls in brain slices of the same region. (b) Quantification of the fluorescence signal ratio left/right for the hippocampal region. (c) Quantification of the fluorescence signal ratio left/right for the substantia nigra. Significance levels: \*/\*\* 6-OHDA vs. vehicle, #/## 6-OHDA/vehicle vs. healthy control; \*/# P < 0.05, \*\*/## P < 0.01; Mann-Whitney Rank Sum Test. Box plot shows median value and upper/lower quartiles. Whiskers display minimal and maximal values obtained.

**Figure 4: Intra-individual time course of BBB leakage:** The intra-individual time course of T1w MRI signal with Gadovist<sup>®</sup> is shown for four animals per group at day 2, 14, and 28. EB *ex vivo* FRI was measured on day 28 and shows slice 3 from posterior (FRI A) and slice 2 from anterior (FRI B) and posterior (FRI C). FRI B corresponds best to the MRI image.

**Figure 5: Areas of increased BBB permeability show increased density and activation of Iba1<sup>+</sup> immune cells:** IgG (IgG), tyrosine hydroxylase (TH), and ionized calcium-binding adapter molecule 1 (Iba1) immunoreactivity in 6-OHDA- and vehicleinjected animals at day 14 and 28 post injection. Scale bar: 200 μm. Figure 6: Parallel Bioluminescence Imaging and blood brain barrier assessment in Dcx-Luc mice after intranigral vehicle injection: (a) Experimental design. (b) Representative BLI images. (c-e) Quantification of BLI signal left/right ratios for OB, SVZ and hippocampus (Mann-Whitney Rank Sum Test). (f) Representative images of in vivo Gadovist<sup>®</sup> enhanced T1w MRI, EB FRI, and IgG staining. (g-h) Quantification of FRI left/right ratios for hippocampus and SN (Wilcoxon Signed Rank Test). Significance level \* P < 0.05, Box plots show median value and upper/lower quartiles. Whiskers display minimal and maximal values obtained.





This article is protected by copyright. All rights reserved.

а



